ANALYTICAL AND NUMERICAL STUDY OF THE INFLUENCE OF DIFFERENT SUPPORT TYPES IN THE NONLINEAR VIBRATIONS OF BEAMS

A. Rincón-Casado[1], J. González-Carbajal[2], D. García-Vallejo[2], J. Domínguez[2]

[1] Department of Mechanical Engineering and Industrial Design, University of Cadiz, 11519, Puerto Real, Spain.

[2] Department of Mechanical Engineering and Manufacturing, Universidad de Sevilla, C/ Camino de los Descubrimientos s/n, 41092 Seville, Spain.

Correspondig author: alejandro.rincon@uca.es

email: alejandro.rincon@uca.es, jgcarbajal@us.es, dgvallejo@us.es, jaime@us.es,

ABSTRACT

As it is well known, , beams vibrations with large oscillations cause nonlinear effects. One of the main observed nonlinear effects is the dependence of the natural frequencies on the amplitude, what is usually represented with backbone curves showing either a softening or a hardening behaviour, being such softening or hardening behaviour highly dependent on the boundary conditions. This paper aims at studying the influence of the different support types on the vibration frequency of a beam, both by analytical and numerical approaches. First, an analytical study of two cases of simply supported beams is carried out by using the nonlinear normal modes (NNM) and the multiple scale methods to obtain the analytical expressions of the nonlinear frequencies as a function of the vibration amplitude. Such results have been compared and discussed with other authors' results. In addition, a nonlinear finite element model of these two cases showed that the analytical and numerical results are in good agreement. Additionally, several numerical studies have been carried out for different support types. A total of seven different boundary conditions have been numerically analysed and the corresponding frequency-amplitude relations have been obtained and compared. In addition, the effect of the axial inertial forces has been enhanced by adding concentrated masses at one end of the beam. It was found for instance that the pinned-pinned beam shows a hardening behaviour, which depends on the beam slenderness, or that the pinned-roller beam results in the largest softening behaviour. The fundamental causes of nonlinearity are, on one hand the coupling of the midline deformation and bending and, on the other hand, the coupling of axial inertial forces and bending. The significance of the first of these effects depends on the beam material and geometrical properties.

Keywords: nonlinear normal modes, nonlinear oscillations, simply supported beam, multiple time scales method

1. Introduction

The demand for enhancing the dynamic performance of structures in terms of weight, comfort, safety, noise and durability continuously increases. At the same time, there is a demand for longer operating life, minimisation of inspection and maintenance, and cost reduction. Such structural elements may be beams subjected to dynamic loads, for example, of aircraft (propellers, wings, etc.), high speed rotors, or superstructure elements. A beam is a basic element in any real structure and its dynamic behaviour may influence that of the complete structure. A real beam does not always behave linearly, that is, in the linear regime. When the vibration amplitudes achieve significant values, an increase or decrease in the natural frequency as compared with the linear frequency can be observed. There are two main causes for the mentioned nonlinear behaviour: the coupling of midline stretching with bending and the coupling of axial inertial forces with bending, being both effects extensively studied in the literature. As it is known, the type of support of the vibration of a beam influences such nonlinear effects. To understand the described dynamical behaviour, an analytical and numerical study is carried out in order to show the effect of the type of support on non-linear frequencies when the amplitude of vibration is large enough.

The main goal of this work is to analyse the effect of different boundary conditions on the nonlinear frequency-amplitude relationship of beams vibrating with large amplitudes. It has been carried out using two approaches. On the one hand, the development of an analytical solution for the nonlinear differential equation of motion for the pinned-roller and the roller-roller beam. The Nonlinear Normal Modes (NNMs) and the multiple scales methods have been used on that purpose. In order to make clear the mathematical approach many details are given. On the other hand, a finite element numerical study of beam vibration in the nonlinear regime is carried out for seven cases with different support types. Previously, the numerical procedure has been validated by comparison with the results of the analytical models. A concluding plot is included in which the hardening and softening behaviours are visible with the help of the backbone natural frequency curves.

The analytical treatment of beam problems allows finding a relation between nonlinear frequency and amplitude for the different modes of vibration of the beam. In the context of analytical methods, different authors have contributed to the study of beam large oscillations, in particular of the unsymmetrical case of a pinned-roller beam. For instance, Thomsen [1] and Han [2] used an Eulerian description of the motion in which time and horizontal position in the deformed beam were utilized as independent variables. In their work, the longitudinal inertia was neglected a priori. In addition, Lacarbonara [3] obtained an integro-differential equation in terms of the transverse deflection depending both on geometric and inertial terms. On the other hand, the symmetrical case of the roller-roller beam has been less extensively studied in the literature, where the numerical analyses performed by Woodall [4] are remarkable. He obtained a softening behavior by using Galerkin and finite differences methods, and a hardening behavior, which shows a very good accordance with the results of the present work, by means of a perturbation technique. Woodall [4] suggests that his perturbation solution might not be accurate enough, because it is out of tune with the other two results. However, the difference between the three approaches is most likely attributed to the formulation of the boundary conditions. Atluri [5] did evaluate the nonlinear inertial term in the simply supported unsymmetrical case (pinned-roller) as proposed in the present work, but arrived at a different expression for the geometric term. This was due to a less detailed formulation of the equilibrium equations, as it was already pointed out by Lungo in [6].

The analytical treatment used in this research is based on the concept of Nonlinear Normal Modes (NNMs). The procedure proposed by Nayfeh [7]-[8] for obtaining the NNMs of beams has also been used in the present work, too. The NNMs introduced by Rosenberg in the 60s [9] has experienced a great development since 1990 due to the works of Shaw and Pierre [10], Vakakis [11], etc. In short, for an unforced conservative system, a NNM can be defined as a family of periodic motions which occur onto a 2D invariant manifold in the phase space of the system. This manifold passes through a stable equilibrium point and, at that point, is tangent to one of the Linear Normal Modes (LNMs) of the linearized system. Then, NNMs are a natural generalization of LNMs, suitable to Nonlinear Systems. For a detailed exposition on NNMs, the reader is referred to [12]. The most straightforward definition of NNM is a vibration in unison of the system (i.e., a synchronous oscillation).

The recent work by Kloda et al. [13] presents analytical and numerical results for a beam with an elastic boundary condition modeled by using a spring. This work carries out a study of the effect of the spring stiffness on the non-linear frequencies. In the analytical study, they used the multiple scales method to obtain an analytical solution, too. In addition, they include a FEM numerical study in which, the system frequency response is obtained by modifying the frequency of the forcing excitation until the system resonates. This methodology has been inspirational for the present work since it is very intuitive, although it presents a certain level of uncertainty and a large computational cost. The present work proposes a similar FEM methodology in which the beam is released from the deformed shape that corresponds to the first linear mode of vibration and it is left to vibrate freely. Then the frequency of the free bending vibration is measured directly on the response.

The paper is organized as follows. Section 2 introduces the material and methods for the analytical and numerical study. The analytical study includes the beam model description, and the application of the NNM and the multiple time scales methods. The numerical analysis procedure is also included in this section. Section 3, shows and discusses the results. On the one hand, the comparison between analytical and numerical results is treated; and on the other hand, the comparison between the seven studied cases with different types of support is treated. Finally, Section 4 shows the main conclusions of this work based on the results obtained.

2. Material and methods

This section describes the beam model studied and the hypotheses considered. Subsequently, the equation of motion is discretized by using the NNMs, the multiple time scales method is applied, eliminating secular terms and obtaining the analytical solution for two cases of simply supported beams (pinned-roller and roller-roller). Finally, the finite element procedure followed for the identification of the nonlinear vibration frequency of the seven cases with different types of support is described. The analytical developments are used in this section to validate the numerical procedure.

2.1 Analytical study

2.1.1 Beam model equation

The equation of motion of the beam is obtained with the following assumptions

- The beam is initially straight, with a uniform cross section.
- The beam experiences planar motion.
- During the motion plane sections remain plane.
- Shear deformations and rotational inertia of the cross section are negligible.
- Strains are small and the material shows a linear elastic behavior.
- No damping or external excitation are considered.

Since shear deformations are not considered, the cross-section angular rotation coincides with rotation of the beam's midline. The beam has initial length, L, constant cross-section area, A, and constant moment of inertia of the beam's cross-section, I. In addition, the beam is homogeneous with a constant Young modulus, E, a shear modulus, G, and a mass density per unit length, ρ. Fig. 1a) shows a section, refereed as 1, without deformation and a section named 2, representing the same cross-section after deformation. In the figure, M, N and Q are bending moment, axial and shear forces, respectively. Internal forces N and Q can be projected onto the global frame in terms of a horizontal and a vertical components (H and V). The displacement in X direction (global frame) is defined as u, the displacement in the Y direction is defined as v, and the elongation of the midline is defined as s. Angular variable θ represents the angle rotated by the cross-section. The equilibrium equations in horizontal and vertical directions, together with the moment equilibrium equation are, respectively:

$$\rho A\ddot{u} = (N\cos\theta)' - (Q\sin\theta)' \tag{1}$$

$$\rho A\ddot{v} = (N\sin\theta)' + (Q\cos\theta)' \tag{2}$$

$$M' + Qs' = 0 \tag{3}$$

where a lagrangian description is assumed, a prime corresponds to spatial derivatives with respect to X, while a dot denotes a partial derivative with respect to time t.

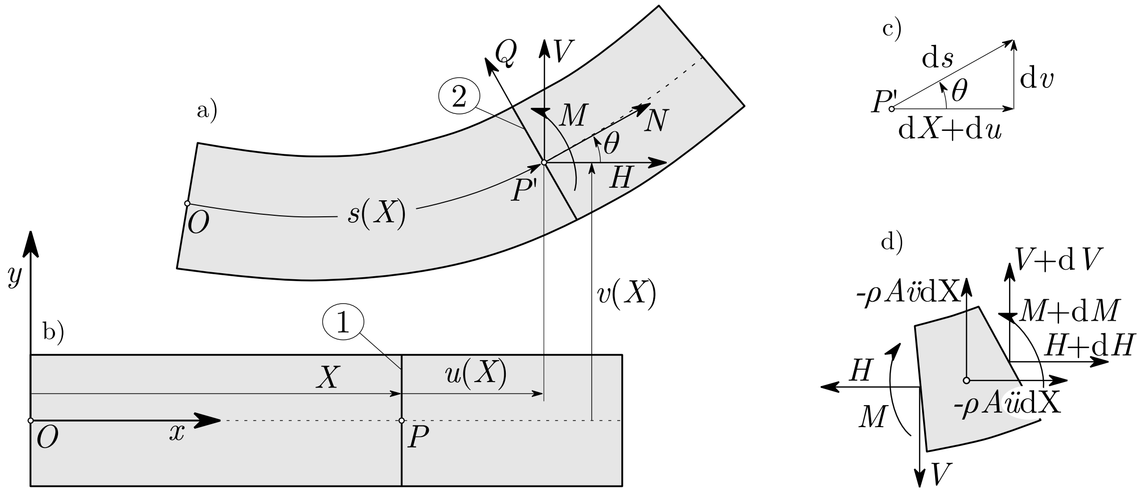

Fig. 1 Forces and displacements at the beam cross-section a) undefordmed beam; b) deformed beam; c) midline elongation; d) equilibrium of an infinitesimal section.

Assuming a linear elastic constitutive model, the following axial and bending relations can be used:

$$N = EA(s' - 1) \tag{4}$$

$$M = EI\theta' \tag{5}$$

Then problem is closed with the addition of the following appropriate geometric relations. According to Fig. 1b), the elongation of the beam midline yields the following relations:

$$\begin{Bmatrix} \sin\theta = v'/s' \\ \cos\theta = (1+u')/s' \end{Bmatrix} \Rightarrow (s' - 1) \approx u' + \frac{1}{2}\left(u'^2 + v'^2\right) \tag{6}$$

$$\frac{\partial\theta}{\partial s} = \frac{\partial^2 v/\partial s^2}{1 + \partial u/\partial s} \Rightarrow \theta' \approx \frac{v''}{1+u'} \tag{7}$$

Combining the previous equations, one gets:

$$\rho A\ddot{u} = N'(1+u') - Q'v' - \frac{v''}{1+u'}[Nv' + Q(1+u')] \tag{8}$$

$$\rho A\ddot{v} = N'v' + Q'(1+u') + \frac{v''}{1+u'}[N(1+u') - Qv'] \tag{9}$$

$$M' + Qs' = 0 \tag{10}$$

$$N = EA\left[u' + \frac{1}{2}(u'^2 + v'^2)\right] \tag{11}$$

$$M = EI\frac{v''}{1+u'} \tag{12}$$

which is a nonlinear system of 5 equations in partial derivatives with 5 unknown functions $u(X,t), v(X,t),\ N(X,t), Q(X,t), M(X,t)$. The previous system of equations was simplified by using that $sin\theta \approx v'$, $cos\theta \approx 1+u'$ and $s' \approx 1$.

2.1.2 Equations of the pinned-roller simply supported beam

The system (8)-(12) needs 6 boundary conditions and 4 initial conditions, $u(X,0), v(X,0), \dot{u}(X,0), \dot{v}(X,0)$. It is valid for arbitrarily large deflections and for any boundary conditions.

At this point, the assumption of moderately large deflections is introduced. This allows for two new simplifications,

- $u'^2 \ll v'^2 \Rightarrow s' - 1 \approx u' + v'^2/2$ and,
- only nonlinearities up to order three will be considered.

Moreover, for beams with unrestrained axial displacements, it is usual to assume the middle line of the beam to be inextensional [6], [5], [3] and [7]. This is analogous to the Euler-Bernoulli assumption of shear strains being negligible, which is also being used here. Let us stress that neglecting axial deformations does not mean neglecting the axial force N. Rather, it is being assigned an infinite value to the axial stiffness EA, so that the axial force can take the necessary value to maintain the beam equilibrium. Once these additional assumptions have been made, it is convenient to rewrite equations (8)-(12) in terms of forces H and V, see the equilibrium of an infinitesimal section of the beam in Fig. 1c):

$$\rho A\ddot{u} = H' \tag{13}$$

$$\rho A\ddot{v} = V' \tag{14}$$

$$M' + V(1+u') - Hv' = 0 \tag{15}$$

$$M = EI\frac{v''}{1+u'} \tag{16}$$

$$u' = -\frac{v'^2}{2} \tag{17}$$

Dividing Equations (15) by $(1+u')$ and deriving Equations (15) and (16) with respect to X, using relation (17), it is possible combine both results with Equation (14) to obtain

$$[M'/(1+u')]' + V' - [Hv'/(1+u')]' = 0 \tag{18}$$

Which leads to

$$\left[\frac{EI\left(\frac{v''}{1-\frac{v'^2}{2}}\right)'}{1-\frac{v'^2}{2}}\right]' + \rho A\ddot{v} - \left[H\frac{v'}{1-\frac{v'^2}{2}}\right]' = 0 \tag{19}$$

It is possible to expand the nonlinear terms as Taylor series, retaining only terms up to order 3. In the same way, order 2 has been selected for horizontal force H.

$$\frac{1}{1-\frac{v'^2}{2}} = 1 + \frac{v'^2}{2} + \frac{v'^4}{4} \approx 1 + \frac{v'^2}{2} \tag{20}$$

What leads to

$$\begin{aligned} EI\left[\frac{\left(\frac{v''}{1-\frac{v'^2}{2}}\right)'}{1-\frac{v'^2}{2}}\right]' &= EI\left[\left(v''(1+\frac{v'^2}{2})\right)'(1+\frac{v'^2}{2})\right]' = \\ &= EI\left[\left(1+v'^2+\frac{1}{4}v'^4\right)v^{IV} + v'''(4v'v''+2v'^3v'') + v''^3\right] \\ &\approx EI[(1+v'^2)v^{IV} + 4v'v''v''' + v''^3] = EI[v^{IV} + [v'(v'v'')']'] \end{aligned} \tag{21}$$

Where it was used that

$$\left[H\frac{v'}{1-\frac{v'^2}{2}}\right]' = \left[Hv'(1+\frac{v'^2}{2})\right]' = [Hv']' + [Hv']'\frac{v'^2}{2} + Hv'v'' \approx [Hv']' \tag{22}$$

Including the previous terms in the equation **¡Error! No se encuentra el origen de la referencia.**, one gets

$$\rho A\ddot{v} + EI[v^{IV} + [v'(v'v'')']'] - [Hv']' = 0 \tag{23}$$

In order to attain an equation where the only unknown is $v(X,t)$, it is required to write H as a function of v, as follows (where z and y are internal variables for the integration)

$$H' = \rho A\ddot{u} \tag{24}$$

$$\ddot{u}' = \frac{\partial^2}{\partial t^2}\left[-\frac{v'^2}{2}\right] = -(v'\ddot{v}' + \dot{v}'^2) \Rightarrow \ddot{u} = \int_0^z (v'\ddot{v}' + \dot{v}'^2)dy \tag{25}$$

$$H = -\rho A\int_L^X \int_0^z (v'\ddot{v}' + \dot{v}'^2)dy\,dz \tag{26}$$

$$[Hv']' = \left[-\rho A v'\int_L^X \int_0^z (v'\ddot{v}' + \dot{v}'^2)dy\,dz\right]' \tag{27}$$

Including the previous terms in Equation (23) the following is achieved

$$\rho A\ddot{v} + EI[v^{IV} + [v'(v'v'')']'] + \left[\rho A v' \int_L^X \int_0^z (v'\ddot{v}' + \dot{v}'^2) dy\, dz\right]' = 0 \tag{28}$$

To simplify the analysis, the following dimensionless parameters are used:

$$v^* = \frac{v}{L}, u^* = \frac{u}{L}, \xi = \frac{X}{L}, \tau = \sqrt{\frac{EI}{\rho A L^4}} t \tag{29}$$

For the sake of simplicity, from now on, a prime will be used for partial derivatives with respect to ξ and a dot will be used for partial derivatives with respect to τ. It will also be omitted the use of the asterisk in v^* and u^*. Although longitudinal displacement u does not appear explicitly in the equation of motion, it will be needed for representing the deformed shapes of the beam.

Then, after combining (28) with the dimensionless parameters in Equation (29), one arrives at

$$\ddot{v} + \frac{EI}{\rho A}[v^{IV} + [v'(v'v'')']'] + \left[v' \int_1^\xi \int_0^\eta (v'\ddot{v}' + \dot{v}'^2) d\gamma\, d\eta\right]' = 0 \tag{30}$$

In order to find a meaningful and simple equation, the following terms are defined:

$$N_G = [v'(v'v'')']' \tag{31}$$

$$N_I = \left[v' \int_1^\xi \int_0^\eta (v'\ddot{v}' + \dot{v}'^2) d\gamma\, d\eta\right]' \tag{32}$$

where N_G is a geometric nonlinear term while N_i is an inertial nonlinear term. Substituting one gets

$$\ddot{v} + v^{IV} + N_G\big(v(\xi,\tau)\big) + N_I\big(v(\xi,\tau)\big) = 0 \tag{33}$$

with boundary conditions

$$v(0,\tau) = v''(0,\tau) = v(1,\tau) = v''(1,\tau) = 0 \tag{34}$$

$$u(0,t) = H(L,t) = 0 \tag{35}$$

Equation (33) highlights the presence of two kinds of nonlinearities in the problem. There exists a geometric term, which does not depend on the longitudinal boundary conditions and an inertial term, which does depend on them. By reviewing the previous mathematical development, it is easy to see the physical meaning of both nonlinear terms. The geometric one comes from the nonlinear expression for the curvature and the fact that the moment arm associated to vertical force V depends on the beam deformation, see Eq. (31). On the other hand, the inertial term comes from the bending moment generated by the horizontal force, H, which in turn is produced by the horizontal inertia of sections, see Eq. (33). An integro-differential equation has been derived for $v(\xi,\tau)$ which is valid for any initial condition $v(\xi,0)$, $\dot{v}(\xi,0)$. In the next section, some important solutions of Eq. (33), namely those corresponding to the NNMs of the beam, are discussed.

2.1.3 Discretization by nonlinear normal modes

The procedure followed by Nayfeh in [7], [8] for obtaining the NNMs of continuous systems has been used to discretize the equations of motion. To this end, displacement v is expanded by means of the linear modes of vibration of the beam and is approximated to an infinite series of linear eigenfunction of the form:

$$v(\xi,\tau)=\sum_{j=1}^{\infty}\phi_j(\xi)q_j(\tau) \tag{36}$$

Note, that the sine function is generally used for simply supported beams by the Rayleigh-Ritz method. The following definition will also be used

$$\phi_j(\xi)=sin(j\pi\xi) \qquad j=1,2,\dots \tag{37}$$

The inner product operator, for continuous functions in ξ between 0 and 1, is defined as:

$$\langle f_1(\xi),f_2(\xi)\rangle=\int_0^1 f_1(\xi)f_2(\xi)\,d\xi \tag{38}$$

Following Galerkin's method, the orthogonality condition for the residual of the differential equation and the space of assumed basis functions results in

$$\langle\phi_j,\ddot{v}\rangle+\langle\phi_j,v^{IV}\rangle+\langle\phi_j,N_G\big(v(\xi,\tau)\big)\rangle+\langle\phi_j,N_I\big(v(\xi,\tau)\big)\rangle=0 \tag{39}$$

As it is well known, linear modes satisfy the next expressions:

$$\begin{gathered}\langle\phi_k(x),\phi_j(x)\rangle=\delta_{kj}/2,\quad \langle\phi_k(x),\phi_j^{IV}(x)\rangle=\omega_j^2\delta_{kj}/2,\\ \omega_j=(k\pi)^2\ ,\omega_k=(k\pi)^2\quad j,k=1,2,\dots\end{gathered} \tag{40}$$

Applying the inner product to each member of Eq. (39) and integrating in ξ, yields

$$\begin{aligned}\langle\phi_j,\ddot{v}\rangle&=\int_0^1\phi_j(\xi)\ddot{v}(\xi,\tau)d\xi=\int_0^1\phi_j(\xi)\sum_{k=1}^{\infty}\phi_k(\xi)\ddot{q}_k(\tau)\,d\xi=\\&=\sum_{k=1}^{\infty}\ddot{q}_k(\tau)\int_0^1\phi_j(\xi)\phi_k(\xi)d\xi=\sum_{k=1}^{\infty}\ddot{q}_k(\tau)\left[\frac{\delta_{kj}}{2}\right]=\frac{\ddot{q}_j(\tau)}{2}\end{aligned} \tag{41}$$

$$\langle \phi_j, v_j^{IV} \rangle = \int_0^1 \phi_j(\xi) v_j^{IV}(\xi,\tau) d\xi = \int_0^1 \phi_j(\xi) (\sum_{k=1}^{\infty} \phi_j^{IV}(\xi) q_k(\tau)) d\xi =$$

$$= \sum_{k=1}^{\infty} q_k(\tau) \int_0^1 \phi_j(\xi) \phi_j^{IV}(\xi) d\xi = \sum_{k=1}^{\infty} q_k(\tau) \left[\frac{\omega_j^2 \delta_{kj}}{2} \right] = q_j(\tau) \frac{\omega_j^2}{2} \qquad (42)$$

Introducing (41) and (42) in (39) one has

$$\frac{\ddot{q}_j}{2} + q_j \frac{\omega_j^2}{2} + G_j = 0, \qquad j = 1,2, \dots \qquad (43)$$

with

$$G_j = 2 \left\langle \phi_j, N_G \left(\sum_{m=1}^{\infty} \phi_m(\tau) q_m(\xi) \right) \right\rangle + 2 \left\langle \phi_j, N_I \left(\sum_{m=1}^{\infty} \phi_m(\tau) q_m(\xi) \right) \right\rangle \qquad (44)$$

Equations (43) are completely equivalent to (33), since any deformed shape of the beam can be expressed as a linear combination of functions ϕ_j. In other words, Equations (43) represent the same problem that Equation (33), but written in modal coordinates. Then, the state of the system at a particular instant is given by variables $q_j, \dot{q}_j$ $(j = 1,2, \dots)$. The main difficulty in Equations (43) is that they are coupled by means of terms G_j, i.e. the evolution of each modal coordinate q_j depends on the rest of them. However, for motions corresponding to a NNM of the beam, with small deflections, this can be overcome. The NNMs of the system are defined as tangent to the linear modes at the equilibrium point given by $v(\xi) = \dot{v}(\xi) = 0$. For the NNM associated to the k-th linear mode, q_k and $\dot{q}_k$ will be used as master variables, the rest being written as functions of them. As a NNM must be tangent to a linear mode, variables $q_j, \dot{q}_j$ $(j \neq k)$ must be functions of order 2 or higher in q_k and $\dot{q}_k$. Actually, they will be shown later to be of order 3. Therefore, for sufficiently small values of q_k and $\dot{q}_k$, G_j can be expanded as

$$G_j = 2 \langle \phi_j, N_G(\phi_k q_k) \rangle + 2 \langle \phi_j, N_I(\phi_k q_k) \rangle + \cdots \qquad (45)$$

where, as usual, the dots represent higher order terms.

Now the terms N_G and N_I will be calculated for k = j where the series of the equation (36) becomes the equation:

$$v(\xi,\tau) = \sum_{j=1}^{\infty} \phi_j(\xi) q_j(\tau) = \phi_k(\xi) q_k(\tau) \qquad (46)$$

The expression for N_G, Equation (31), can be derived to get

$$N_G = [v'(v'v'')']' = v'^2 v^{IV} + 4v'v''v''' + v''^3 \qquad (47)$$

Making the derivatives using Equation (46) and simplifying the notation, where q_k does not depend on ξ and comes out common factor, on gets

$$N_G(\phi_k(\xi)q_k(\tau)) = q_k^3\left[{\phi_k}'^2{\phi_k}^{IV} + 4{\phi_k}'{\phi_k}''{\phi_k}''' + {\phi_k}''^3\right] = \\ = q_k^3[{\phi_k}'({\phi_k}'{\phi_k}'')']' \tag{48}$$

Then, the inner product results in

$$2\langle\phi_j, N_G(\phi_k q_k)\rangle = 2\langle\phi_j, q_k^3[{\phi_k}'({\phi_k}'{\phi_k}'')']'\rangle = q_k^3\, 2\langle\phi_j, [{\phi_k}'({\phi_k}'{\phi_k}'')']'\rangle \\ = q_k^3\, g_{1jk} \tag{49}$$

Where g_{1jk} is defined as

$$g_{1jk} = 2\langle\phi_j, [\phi_k'(\phi_k'\phi_k'')']'\rangle \tag{50}$$

Following a similar approach for term N_I

$$v(\xi,\tau) = \phi_k(\xi)q_k(\tau);\; v' = {\phi_k}'q_k;\; \dot{v}'^2 = {\phi_k}'^2{\dot{q}_k}^2; \ddot{v}' = {\phi_k}'\ddot{q}_k \tag{51}$$

Then, Eq. (32) can be written as

$$N_I = \left[v'\int_1^\xi\int_0^\eta (v'\ddot{v}' + \dot{v}'^2)d\gamma\, d\eta\right]' = \\ = \left[{\phi_k}'q_k\int_1^\xi\int_0^\eta ({\phi_k}'q_k{\phi_k}'\ddot{q}_k + {\phi_k}'^2{\dot{q}_k}^2)d\gamma\, d\eta\right]' \\ = \left(q_k\dot{q}_k^2 + q_k^2\ddot{q}_k\right)\left[\phi_k'\int_1^\xi\int_0^\eta \phi_k'^2 d\gamma\, d\eta\right] \tag{52}$$

The corresponding inner product can be written in terms of q_k as

$$2\langle\phi_j, N_I(\phi_k q_k)\rangle = 2\left\langle\phi_j, \left(q_k\dot{q}_k^2 + q_k^2\ddot{q}_k\right)\left[\phi_k'\int_1^\xi\int_0^\eta \phi_k'^2 d\gamma\, d\eta\right]\right\rangle = \\ = \left(q_k\dot{q}_k^2 + q_k^2\ddot{q}_k\right)\cdot 2\left\langle\phi_j, \left[\phi_k'\int_1^\xi\int_0^\eta \phi_k'^2 d\gamma\, d\eta\right]\right\rangle = \\ = \left(q_k\dot{q}_k^2 + q_k^2\ddot{q}_k\right)\cdot g_{2jk} \tag{53}$$

where g_{2jk} is calculated as

$$g_{2jk} = 2\,\langle \phi_j, \left[\phi_k' \int_1^{\xi} \int_0^{\eta} \phi_k'^2 d\gamma\, d\eta\right]' \rangle \tag{54}$$

The use of terms "large" and "small" is emphasized at this point in order to avoid confusion during the subsequent developments. That is, deflections are being assumed to be large enough for the effect on nonlinearity to be significant, yet small enough for our approximations to work.

Introducing (49) and (53) in (45) yields

$$G_j = g_{1jk} \cdot q_k^3 + g_{2jk} \cdot \left(q_k \dot{q}_k^2 + q_k^2 \ddot{q}_k\right) + \cdots \tag{55}$$

with

$$g_{1jk} = 2\langle \phi_j, [\phi_k'(\phi_k'\phi_k'')']' \rangle \tag{56}$$

$$g_{2jk} = 2\,\langle \phi_j, \left[\phi_k' \int_1^{\xi} \int_0^{\eta} \phi_k'^2 d\gamma\, d\eta\right]' \rangle \tag{57}$$

Next, the terms in Eqs. (54) and (55) are evaluated by carrying out the required derivatives with respect to ξ and the corresponding integration between 0 and 1 leading to the following results

$$\begin{aligned} g_{1jk} &= 2\langle \phi_j, [\phi_k'(\phi_k'\phi_k'')']' \rangle = 2\int_0^1 \phi_k \cdot [\phi_k'(\phi_k'\phi_k'')']' d\xi = \\ &= 2\int_0^1 \phi_k \cdot [{\phi_k}'^2 {\phi_k}^{IV} + 4{\phi_k}'{\phi_k}''{\phi_k}''' + {\phi_k}''^3] d\xi = \frac{(k\pi)^6}{2} \end{aligned} \tag{58}$$

$$\begin{aligned} g_{2jk} &= 2\int_0^1 \phi_k \cdot \left[\phi_k' \int_1^{\xi} \int_0^{\eta} {\phi_k'}^2 d\gamma\, d\eta\right]' d\xi = \\ &= 2\int_0^1 \left[sin(k\pi\xi) \left[(k\pi) cos(k\pi\xi) \int_1^{\xi} \int_0^{\eta} (k\pi)^2 cos^2(k\pi\gamma)\ d\gamma\, d\eta\right]' \right] d\xi = \\ &= \frac{(k\pi)^4}{6} - \frac{3(k\pi)^2}{16} \end{aligned} \tag{59}$$

Substituting equation (55) into (43) and using (58) and (59) one obtains the discretized equation of motion for vibration mode k

$$\ddot{q}_k + \omega_k^2 q_k + \frac{(k\pi)^6}{2} q_k^3 + \left[\frac{(k\pi)^4}{6} - \frac{3(k\pi)^2}{16}\right] \left[q_k \dot{q}_k^2 + q_k^2 \ddot{q}_k\right] = 0 \tag{60}$$

2.1.4 Analytical solution based on the multiple scales methods

This section presents the application of the multiple scale method to solve the nonlinear equation of motion. The nonlinear term is assumed to be weak or small compared to the linear term. The parameter $\varepsilon \ll 1$ has to be introduced in the nonlinear term as follows

$$\ddot{q}_k + \omega_k^2 q_k + \varepsilon\left[\frac{(k\pi)^6}{2} q_k^3 + \left[\frac{(k\pi)^4}{6} - \frac{3(k\pi)^2}{16}\right]\left[q_k \dot{q}_k^2 + q_k^2 \ddot{q}_k\right]\right] = 0 \tag{61}$$

By straightforward expansion, the solution is assumed to be expandable in terms of parameter ε.

$$q_k(\tau) = q_{k0}(\tau) + \varepsilon q_{k1}(\tau) + \varepsilon^2 q_{k2}(\tau) + \cdots \tag{62}$$

As it is known, for large amplitude oscillations the straightforward expansion technique generates secular terms and fails to correctly provide a proper relation between amplitude and frequency. The multiple scales method avoids this shortcoming by allowing a solution to be obtained independently of the time scales. For example, the fast scale can be used for frequencies near to the linear system, while the slow scale for slow modulations of amplitudes and phases. According to the multiple scale method, the solution can be expressed in terms of different time scales, T_0 and T_1 for first order expansion as follows.

$$\begin{gathered} q_k(T_0, T_1) = q_{k0}(T_0, T_1) + \varepsilon q_{k1}(T_0, T_1) + \cdots \\ T_0 = \tau, T_1 = \varepsilon\tau, \quad \varepsilon \ll 1 \end{gathered} \tag{63}$$

$$q = q_0 + \varepsilon q_1 + \cdots \tag{64}$$

$$\dot{q} = D_0 q_0 + \varepsilon D_0 q_1 + \varepsilon D_1 q_0 \tag{65}$$

$$\ddot{q} = D_0^2 q_0 + \varepsilon D_0^2 q_1 + 2\varepsilon D_0 D_1 q_0 \tag{66}$$

Equations (64), (65) and (66) show the displacement, velocity and acceleration, respectively, where D_0 and D_1 denote the derivate respect to T_0 and T_1 respectively. Including Equations (64), (65) and (66) into equation (61), one has

$$\begin{bmatrix} (D_0^2 q_0 + \varepsilon D_0^2 q_1 + 2\varepsilon D_0 D_1 q_0) + \\ +\omega_k^2 (q_0 + \varepsilon q_1) + \varepsilon \dfrac{(k\pi)^6}{2} (q_0 + \varepsilon q_1)^3 + \\ +\varepsilon\left[\dfrac{(k\pi)^4}{6} - \dfrac{3(k\pi)^2}{16}\right]\begin{bmatrix} (q_0 + \varepsilon q_1)[D_0 q_0 + \varepsilon D_0 q_1 + \varepsilon D_1 q_0]^2 + \\ (q_0 + \varepsilon q_1)^2 [D_0^2 q_0 + \varepsilon D_0^2 q_1 + 2\varepsilon D_0 D_1 q_0] \end{bmatrix} \end{bmatrix} = 0 \tag{67}$$

According to Equation (64), it is necessary to obtain q_0 and q_1. To obtain q_0, $\varepsilon = 0$ is assumed in equation (67), obtaining the following homogeneous differential equation

$$\ddot{q}_k + \omega_k^2 q_k + 0 = 0 \tag{68}$$

$$q = q_0; \ \dot{q} = D_0 q_0; \ \ddot{q} = D_0^2 q_0 \tag{69}$$

$$D_0^2 q_0 + \omega_k^2 q_0 = 0 \tag{70}$$

with harmonic solution as follows

$$q_0 = a_k \, cos(\omega_k T_0 + \varphi_k) \tag{71}$$

This solution can be expressed in complex notation as follows

$$q_{0k} = A(T_1)e^{i\omega_k T_0} + \bar{A}(T_1)e^{-i\omega_k T_0} \tag{72}$$

For the first order solution (q_1) the terms of order zero are eliminated leading to

$$\begin{bmatrix} D_0^2 q_1 + \omega_k^2 q_1 - 2D_0 D_1 q_0 - \dfrac{(k\pi)^6}{2} q_0^3 + \\ + \left[\dfrac{(k\pi)^4}{6} - \dfrac{3(k\pi)^2}{16}\right][q_0(D_0 q_0)^2 + (q_0)^2(D_0^2 q_0)] \end{bmatrix} = 0 \tag{73}$$

Using the linear solution for q_0, Eq. (73) can be further developed. In what follows, some important terms are presented, where *cc* denotes de complex conjugates.

$$-2D_0 D_1 q_0 = -2i\omega_k A' e^{i\omega_k T_0} + cc \tag{74}$$

$$-\frac{(k\pi)^6}{2}(q_0)^3 = -\frac{(k\pi)^6}{2}(A^3 e^{i3\omega_k T_0} + 3A^2 \bar{A} e^{i\omega_k T_0} + cc) \tag{75}$$

$$(q_0)(D_0 q_0)^2 + (q_0)^2(D_0^2 q_0) = -2A^3 \omega_k^2 e^{i3\omega_k T_0} - 2A^2 \bar{A} \omega_k^2 e^{i\omega_k T_0} + cc \tag{76}$$

Including the previous terms in equation (73) one finds

$$\begin{bmatrix} D_0^2 q_1 + \omega_k^2 q_1 - 2i\omega_k A' e^{i\omega_k T_0} + cc - \\ -\dfrac{(k\pi)^6}{2}\left(A^3 e^{i3\omega_k T_0} + 3A^2 \bar{A} e^{i\omega_k T_0} + cc\right) + \\ + \left[\dfrac{(k\pi)^4}{6} - \dfrac{3(k\pi)^2}{16}\right]\left(-2A^3 \omega_k^2 e^{i3\omega_k T_0} - 2A^2 \bar{A} \omega_k^2 e^{i\omega_k T_0} + cc\right) \end{bmatrix} = 0 \tag{77}$$

2.1.4.a Elimination of secular terms

In Equation (77) the so-called secular terms are identified because they include the factor $e^{i\omega_k T_0}$. These terms must be eliminated to avoid resonant terms in the solution. From Equation (75), the coefficient of the secular terms is written as follows

$$-2i\omega_k A' - \frac{(k\pi)^6}{2}(3A^2 \bar{A}) + \left[\frac{(k\pi)^4}{6} - \frac{3(k\pi)^2}{16}\right]\left(2A^2 \bar{A} \omega_k^2\right) = 0 \tag{78}$$

$$A = \tfrac{1}{2} a_k e^{j\varphi}, a_k(T_1), \varphi_k(T_1) \in \mathbb{R} \tag{79}$$

Note that the complex amplitude, *A*, of the zero order solution has been expressed in terms of a real amplitude and a real offset angle both depending on T_1. Including these terms in Equation (78) one gets the following

$$-2i\omega_k\left(\tfrac{1}{2}a_k' e^{j\varphi} + \tfrac{1}{2}a_k i\varphi_k' e^{j\varphi_k}\right) - \tfrac{(k\pi)^6}{2}\left(3\left(\tfrac{1}{2}a_k e^{j\varphi_k}\right)^2\left(\tfrac{1}{2}a_k e^{-j\varphi_k}\right)\right) + \\ + \left[\tfrac{(k\pi)^4}{6} - \tfrac{3(k\pi)^2}{16}\right]\left(2\left(\tfrac{1}{2}a_k e^{j\varphi_k}\right)^2\left(\tfrac{1}{2}a_k e^{-j\varphi_k}\right)\omega_k^2\right) = 0 \qquad (80)$$

Equation (80) is further simplified as follows

$$-a_k' i\omega_k - i^2 a_k\varphi_k'\omega_k - \frac{(k\pi)^6}{2}\frac{3}{8}a_k^3 + \left[\frac{(k\pi)^4}{6} - \frac{3(k\pi)^2}{16}\right]\left(\frac{2}{8}a_k^3\right)\omega_k^2 = 0 \qquad (81)$$

Both the real and imaginary parts of the previous equation must be equal to zero, leading to the following relations

$$-a_k' i\omega_k = 0 \Rightarrow a_k = a_{k0} \qquad (82)$$

$$a_k\varphi_k'\omega_k - 3\frac{(k\pi)^6}{16}a_k^3 + \frac{1}{4}\left[\frac{(k\pi)^4}{6} - \frac{3(k\pi)^2}{16}\right]a_k^3\omega_k^2 = 0 \qquad (83)$$

Note that Equation (82) is fulfilled if a_k is constant. On the other hand, Equation (83) leads to the following

$$a_k\varphi_k' - 3\frac{(k\pi)^6}{16}\frac{a_k^3}{\omega_k} + \frac{1}{4}\left[\frac{(k\pi)^4}{6} - \frac{3(k\pi)^2}{16}\right]a_k^3\omega_k = 0 \qquad (84)$$

Substituting $a_k = a_{k0}$ and $\omega_k = (k\pi)^2$ into Equation (84) and integrating in T_1, the offset angle can be found as follows

$$\varphi_k' = 3\frac{(k\pi)^6}{16(k\pi)^2}a_{k0}^2 - \frac{1}{4}\left[\frac{(k\pi)^4}{6} - \frac{3(k\pi)^2}{16}\right]a_{k0}^2(k\pi)^2 \qquad (85)$$

that can be further simplified as

$$\varphi_k' = 3\frac{4}{4}\frac{(k\pi)^4}{16}a_{k0}^2 - \frac{1}{4}\frac{(k\pi)^6}{6}a_{k0}^2 + \frac{3}{4}\frac{(k\pi)^4}{16}a_{k0}^2 \qquad (86)$$

$$\varphi_k' = \left[\frac{15(k\pi)^4}{64} - \frac{(k\pi)^6}{24}\right]a_{k0}^2 \qquad (87)$$

which after integration provides the phase angle as a function of T_1 as

$$\varphi_k = \varphi_{k0} + \left[\frac{15(k\pi)^4}{64} - \frac{(k\pi)^6}{24}\right]a_{k0}^2 T_1 \qquad (88)$$

2.1.4.b Solution of the first order of ε

Once the secular terms are eliminated, Equation (77) reads as follows

$$\begin{bmatrix} D_0^2 q_1 + \omega_k^2 q_1 - \frac{(k\pi)^6}{2}\left(A^3 e^{i3\omega_k T_0}\right) + \\ + \left[\frac{(k\pi)^4}{6} - \frac{3(k\pi)^2}{16}\right]\left(2A^3 \omega_k^2 e^{i3\omega_k T_0}\right) + cc \end{bmatrix} = 0 \tag{89}$$

To solve the previous equation, the following harmonic test solution will be used

$$q_1 = B(T_1) e^{i3\omega_k T_0} + cc \tag{90}$$

which has to be differentiated and substituted into Equation **¡Error! No se encuentra el origen de la referencia.** leading to

$$\begin{bmatrix} -9\omega_k^2 B(T_1) e^{i3\omega_k T_0} + \omega_k^2 B(T_1) e^{i3\omega_k T_0} - \frac{(k\pi)^6}{2}\left(A^3 e^{i3\omega_k T_0}\right) \\ + \left[\frac{(k\pi)^4}{6} - \frac{3(k\pi)^2}{16}\right]\left(2A^3 \omega_k^2 e^{i3\omega_k T_0}\right) + cc \end{bmatrix} = 0 \tag{91}$$

Dividing by $\omega_k^2 e^{i3\omega_k T_0}$ and substituting $\omega_k = (k\pi)^2$ one finds $B(T_1)$ as follows

$$-8B(T_1) = -\frac{1}{\omega_k^2}\frac{(k\pi)^6}{2}(A^3) + \left[\frac{(k\pi)^4}{6} - \frac{3(k\pi)^2}{16}\right](2A^3) + cc \tag{92}$$

that leads to

$$\begin{aligned} B(T_1) &= \left[\frac{1}{8}\frac{1}{(k\pi)^4}\frac{(k\pi)^6}{2} - \frac{2}{8}\frac{(k\pi)^4}{6} + \frac{2}{8}\frac{3(k\pi)^2}{16}\right]A^3 + cc = \\ &= \left[\frac{8}{8}\frac{1}{8}\frac{(k\pi)^2}{2} - \frac{(k\pi)^4}{24} + \frac{6}{8}\frac{(k\pi)^2}{16}\right]A^3 + cc = \\ &= \left[\frac{7(k\pi)^2}{64} - \frac{(k\pi)^4}{24}\right]A^3 + cc \end{aligned} \tag{93}$$

Including $B(T_1)$ in

$$\begin{gathered} q_1 = B(T_1) e^{i3\omega_k T_0} + cc \\ A = \tfrac{1}{2} a e^{j\varphi} \end{gathered} \tag{94}$$

one gets q_1 as follows

$$
\begin{aligned}
q_1 &= \left[\frac{7(k\pi)^2}{64} - \frac{(k\pi)^4}{24}\right] A^3 e^{i3\omega_k T_0} + cc = \\
&= \left[\frac{7(k\pi)^2}{64} - \frac{(k\pi)^4}{24}\right] \frac{1}{8} a_k^3 e^{3j\varphi} e^{i3\omega_k T_0} + cc = \\
&= \left[\frac{7(k\pi)^2}{256} - \frac{(k\pi)^4}{96}\right] a_k^3 e^{3j\varphi} e^{i3\omega_k T_0} + cc = \\
&= \left[\frac{7(k\pi)^2}{256} - \frac{(k\pi)^4}{96}\right] a_k^3 \, cos(3(\omega_k \tau + \varphi_k))
\end{aligned} \tag{95}
$$

Considering $\varepsilon = 1$ and substituting q_0 from Equation (71), q_1 from Equation (95), and φ_k from Equation (88) in the general solution one obtains

$$
\begin{gathered}
q(\tau, \varepsilon) = q_0 + \varepsilon q_1 \\
\varepsilon = 1, \tau = T_0 = T_1
\end{gathered} \tag{96}
$$

Where

$$
q_0 = a_k cos(\omega_k \tau + \varphi_k) \tag{97}
$$

$$
\varphi_k = \varphi_{k0} + \left[\frac{15(k\pi)^4}{64} - \frac{(k\pi)^6}{24}\right] a_{k0}^2 \tau \tag{98}
$$

Thus, the mathematical expression of $q_k(\tau)$ reads as follows

$$
q_k(\tau) = a_k \, cos(\omega_k \tau + \varphi_k) + \left[\frac{7(k\pi)^2}{256} - \frac{(k\pi)^4}{96}\right] a_k^3 \, cos(3(\omega_k \tau + \varphi_k)) \tag{99}
$$

which can be further simplified, leading to

$$
\begin{aligned}
q_k(\tau) &= a_k \, cos\left(\omega_k \tau + (\varphi_{k0} + \left[\frac{15(k\pi)^4}{64} - \frac{(k\pi)^6}{24}\right] a_{k0}^2 \tau)\right) + \\
&+ \left[\frac{7(k\pi)^2}{256} - \frac{(k\pi)^4}{96}\right] a_k^3 \, cos\left(3(\omega_k \tau + (\varphi_{k0} + \left[\frac{15(k\pi)^4}{64} - \frac{(k\pi)^6}{24}\right] a_{k0}^2 T_1))\right)
\end{aligned} \tag{100}
$$

The nonlinear frequency of the system is identified within the argument of the cosine function as follows

$$
\omega_{kNL} \tau = \omega_k \tau + \left[\frac{15(k\pi)^4}{64} - \frac{(k\pi)^6}{24}\right] a_{k0}^2 \tau \tag{101}
$$

Note that the mathematical expression of the nonlinear frequency will be different for different boundary conditions. Substituting in the general equation we have

$$
q_k(\tau) = a_k \, cos(\omega_{kNL} \tau + \varphi_{k0}) + \left[\frac{7(k\pi)^2}{256} - \frac{(k\pi)^4}{96}\right] a_k^3 \, cos(3(\omega_{kNL} \tau + \varphi_{k0})) \tag{102}
$$

Dividing Equation (97) by τ and ω_k, one gets the relationship between linear and nonlinear frequency is obtained

$$\frac{\omega_{kNL}}{\omega_k} = 1 + \left[\frac{15(k\pi)^2}{64} - \frac{(k\pi)^4}{24}\right] a_{k0}^2 \tag{103}$$

where a_k and φ_{k0} are constants that depend on the initial conditions for first order approximations to the amplitude and phase of the motion.

In addition, substituting Equation (55) into Equation (43) for $j \neq k$ yields

$$\begin{gathered} \ddot{q}_j + \omega_j^2 q_j + g_{1jk} q_k^3 + g_{2jk}\left(q_k \dot{q}_k^2 + q_k^2 \ddot{q}_k\right) + \cdots = 0 \\ j \neq k \end{gathered} \tag{104}$$

In order to solve (104) note that, if it is multiplied by q_k^2, one gets $q_k^2 \ddot{q}_k = -\omega_k^2 q_k^3 + \cdots$. On the other hand, by definition of NNM, variables $q_j, \dot{q}_j$ $(j \neq k)$ must be functions of q_k and $\dot{q}_k$. Thus, solutions of Equation (104) of the form

$$q_j = \Gamma_{1jk} q_k^3 + \Gamma_{2jk} q_k \dot{q}_k^2 + \cdots, \qquad j \neq k \tag{105}$$

are sought where Γ_{1jk} and Γ_{2jk} are constants ([7], [8]). Introducing Equation (105) in (104) yields

$$\left\{\begin{aligned} \Gamma_{1jk} &= \frac{\left(7\omega_k^2 - \omega_j^2\right) g_{1jk} - \left(5\omega_k^2 - \omega_j^2\right) \omega_k^2 g_{2jk}}{\left(\omega_k^2 - \omega_j^2\right)\left(9\omega_k^2 - \omega_j^2\right)} \\ \Gamma_{2jk} &= \frac{6 g_{1jk} - \left(3\omega_k^2 + \omega_j^2\right) g_{2jk}}{\left(\omega_k^2 - \omega_j^2\right)\left(9\omega_k^2 - \omega_j^2\right)} \end{aligned}\right\} \; j \neq k \tag{106}$$

The expressions in Equation (106) suggests that this approach fails at one-to-one or three-to-one internal resonances. Hence, it will be assumed that the values of ω_j are away from ω_k and $3\omega_k$. Finally, the expression for the k-th NNM is reconstructed as follows

$$\begin{gathered} v(\xi, \tau) = \phi_k(\xi) q_k(\tau) + \\ \sum_{j \neq k} \phi_j(\xi) \Gamma_{1jk} q_k^3(\tau) + \sum_{j \neq k} \phi_j(\xi) \Gamma_{2jk} q_k(\tau) \dot{q}_k^2(\tau) + \cdots \end{gathered} \tag{107}$$

2.1.5 Nonlinear frequency of a roller-roller simply supported beam

Using a similar procedure, the nonlinear oscillations of the roller-roller simply supported beam can be analyzed. To do that, one has to modify accordingly the axial boundary conditions previously used in the pinned-roller case. This time the axial reaction force at both beam ends vanish

$$H(0, t) = H(L, t) = 0 \tag{108}$$

Therefore, the axial displacement of the previously pinned beam end is released and, therefore, $u(0, t)$ does not need to be zero. Following Equations (23) and (24), the axial force $H(X, t)$ can be evaluated as follows

$$H = \begin{Bmatrix} -\rho A \int_L^X \int_0^z (v'\ddot{v}' + \dot{v}'^2) dy\, dz + \\ +\rho A \frac{(X-L)}{L} \int_0^L \int_0^z (v'\ddot{v}' + \dot{v}'^2) dy\, dz \end{Bmatrix} \tag{109}$$

Note the previous expression fulfills the boundary conditions of Equation (108). As a result of Equation (109), the nonlinear inertial term N_I of Equation (33) is now written as follows

$$N_I = \begin{Bmatrix} \left[v' \int_1^\xi \int_0^\eta (v'\ddot{v}' + \dot{v}'^2) d\gamma\, d\eta \right]' + \\ +[v'(1-\xi)]' \int_0^1 \int_0^\eta (v'\ddot{v}' + \dot{v}'^2) d\gamma\, d\eta \end{Bmatrix} \tag{110}$$

This results in the following expression for g_{2jk}, see Equation (43),

$$g_{2jk} = \begin{Bmatrix} 2 \left\langle \phi_j, \left[\phi_k' \int_1^\xi \int_0^\eta \phi_k'^2 d\gamma\, d\eta \right]' \right\rangle \\ +2 \int_0^1 \int_0^\eta \phi_k'^2 d\gamma\, d\eta \left\langle \phi_j, [\phi_k'(1-\xi)]' \right\rangle \end{Bmatrix} \tag{111}$$

Following a procedure similar to the one described in Section 2.1.4 for the ordinary differential equations of the pinned-roller simply supported case, the following expression is found

$$q_k(\tau) = a_k \cos(\omega_{kNL}\tau + \varphi_{k0}) + \left[\frac{7(k\pi)^2}{256} - \frac{(k\pi)^4}{384} \right] a_k^3 \cos(3(\omega_{kNL}\tau + \varphi_{k0})) \tag{112}$$

Where the expression of the nonlinear frequency is identified as follows

$$\frac{\omega_{kNL}}{\omega_k} = 1 + \left[\frac{15(k\pi)^2}{64} - \frac{(k\pi)^4}{96} \right] a_{k0}^2 \tag{113}$$

2.1.6 Nonlinear frequency of a pinned-pinned beam

The beam with constrained axial displacement at both ends (pinned-pinned) can be analysed following a methodology that is similar to the one used in the previous cases. Assuming that the distance between the pins is equal to the undeformed length of the beam, any deflection necessarily produces stretching of the middle line of the beam. Thus, the assumption of small axial strains restricts the amplitude of deflections

$$|s' - 1| \ll 1 \Rightarrow v'^2 \ll 1, |u'| \ll 1 \tag{114}$$

For clarity, it is emphasized that v'^2 and $|u'|$ were allowed to be large in Sections 2.1.4 and 2.1.5, compensating each other so that $|s' - 1|$ remained small. This is not possible for the axially restrained beam, since u is imposed to vanish at both ends and, therefore, the average contribution of u' to the axial strain is zero. Already Mettler [14] obtained a nonlinear equation of motion for the two axially restrained simply supported beam.

$$\rho A\ddot{v} + EIv^{IV} - \frac{EA}{L}v''\int_0^L \frac{v'^2}{2}dX = 0 \tag{115}$$

Expression (115) can be directly by neglecting all the small terms in the system of Equations (13)-(17) according to (114). The only nonlinear term, of geometric nature, is a hardening type one and accounts for the midline stretching necessarily associated to bending. Applying a procedure similar to the one used in the previous sections to Equation (115) with B.C, previously transformed to dimensionless form by means of (29), one obtains the frequency-amplitude equation for the different NNMs where λ is the slenderness ratio (117)

$$\frac{\omega_{kNL}}{\omega_k} = 1 + \frac{3\lambda^2}{32}a_k^2 + \cdots \tag{116}$$

with

$$\lambda = \frac{L}{\sqrt{I/A}} \tag{117}$$

and, as in Equation **¡Error! No se encuentra el origen de la referencia.**, a_k represents a first order approximation for the amplitude of oscillation of $q_k(\tau)$.

It is convenient, for the following reasoning, to obtain the axial strain ε –averaged over the beam length– when the beam is vibrating along its k-th NNM:

$$\left\{\begin{array}{c} v(\xi,\tau) = q_k(\tau)\, sin(k\pi\xi) \\ \overline{s'-1} = \bar{\varepsilon} = \displaystyle\int_0^1 \frac{v'^2}{2}d\xi \end{array}\right\} \Rightarrow \bar{\varepsilon}(\tau) = \left(\frac{\pi k q_k(\tau)}{2}\right)^2 \tag{118}$$

It has been made use of the fact that, in this particular case, the nonlinear mode shapes coincide with the linear ones [7]. Some authors, while retaining the assumptions of Section 2 of the present paper, have proposed more complex expressions than (115), which include other nonlinearities, such as nonlinear curvature or longitudinal inertia [1,5]. However, it can be shown that these additional terms have the same order of magnitude as the axial strain. Thus, according to the small strains assumption, they would only produce a marginal improvement in the accuracy of the solution.

Luongo et al. [6] derived a model for the axially restrained beam, including the effect of nonlinear curvature. They arrived at equation

$$\frac{\omega_{kNL}}{\omega_k} = 1 + \frac{3\lambda^2}{32}a_k^2 - \frac{3(k\pi)^2}{16}a_k^2 + \cdots \tag{119}$$

Using (118), one can rewrite the last term in (119) as

$$\frac{3(k\pi)^2}{16}a_k^2 = \frac{3}{4}\bar{\varepsilon}_0 \tag{120}$$

where $\bar{\varepsilon}_0$ is a first order approximation for the amplitude of $\bar{\varepsilon}(\tau)$ during the oscillation. Hence, it is clear that, according to the small strains assumption, the last term in (119) can be neglected against unity, which would transform (119) into the expression given by Mettler [14], that is, Equation **¡Error! No se encuentra el origen de la referencia.**.

Lacarbonara [3] also derived a more complex expression than **¡Error! No se encuentra el origen de la referencia.**) for the nonlinear frequencies of the beam, including additional nonlinear terms. In order to understand their results, the nonlinear term in Equation **¡Error! No se encuentra el origen de la referencia.**) is expressed in terms of the axial strain, using Equation (118) as follows

$$\frac{3\lambda^2}{32}a_k^2 = \frac{3}{8}\left(\frac{\lambda}{\pi k}\right)^2 \bar{\varepsilon}_0 \tag{121}$$

Then, for this term to be significant against unity, the coefficient multiplying the axial strain should be considerably greater than one. In their work, Lacarbonara and Yabuno [3] show that their coefficient of nonlinearity Γ_k, defined as

$$\frac{\omega_{kNL}}{\omega_k} = 1 - \Gamma_k a_k^2 + \cdots, \tag{122}$$

becomes significantly different to that of Mettler [14] when $\lambda/(\pi k) \sim 1$, while they are essentially the same for $\lambda/(\pi k) \gg 1$. It is interesting to note that, for $\lambda/(\pi k) \sim 1$ –i.e. moderately slender beams and high modes–, the nonlinear correction given by Mettler's theory in Equation **¡Error! No se encuentra el origen de la referencia.** becomes negligible, according to Equation (121). In fact, there is a nonlinear correction which is, compared to unity, of the order of the axial strain. Therefore, according to the assumption of small strains, the nonlinear effect can be legitimately neglected. Then, for $\lambda/(\pi k) \sim 1$, the nonlinear coefficient obtained in Ref. [3] differs slightly from that of Mettler since the nonlinear correction is very small in any case.

2.2 Numerical study.

The numerical study carried out is divided into two parts. First, the numerical results are validated with the analytical results of the pinned-roller, roller-roller and pinned-pinned beam cases. Second, seven cases of a beam with different types of end supports are solved numerically (see Table 1). The analysis of the results of the cases studied improves the understanding of the influence of the beam support conditions on the nonlinear response of the beam. The numerical study is carried out using Abaqus CAE software.

The beam studied has a length of 500 mm and cross-section of 50 x 50 mm. The mechanical properties of the material used in Abaqus CAE are as follows: Young's modulus E = 210 GPa, Poisson's ratio ν = 0.3 and density ρ = 7850 kg/m^3. The beam geometry is modelled using ten B32 elements beam-type elements with quadratic geometric order uniformly distributed. The frequencies of each vibration mode in the linear models in Abaqus are calculated using the Lanczos method; this method is valid for small displacements. In the case of large oscillations, it is necessary to use beam modelling methods. To do this, an initial displacement is defined in Abaqus, and the displacements at the midpoint of the beam are calculated as the dynamic response to the initial displacements imposed. Additionally, to calculate the nonlinear oscillation frequency, the nonlinear mode "NLgeom" is activated, and Abaqus takes the geometric nonlinearities into account. Conversely, this parameter is deactivated to obtain the linear frequency. To configure the dynamic simulation, it is necessary to define the time increment and the total simulation time. These parameters vary depending on the oscillation frequency of the case studied and can vary between 400-1000 Hz for linear frequencies; however, nonlinear frequencies may be outside this range. In most cases simulated, satisfactory results are obtained with time increments of 10^{-5} s. The simulation time is selected such that at least 10 oscillation cycles are obtained. The response analysed is the displacement at the midpoint of the beam, which is processed with a Fourier transform, yielding the oscillation frequency as a result.

For the numerical study of the influence of the type of end support, seven cases were defined according to the type of constraint at the beam ends (see Table 1). For these cases, it is necessary to know the deflection equation of the first linear mode of vibration and calculate the initial displacement of each node as a function of the studied amplitude. Eq. (123) represents the vertical displacement of each point along the beam as a function of coefficients A, B, C and D [15], which depend on the type of end support, the dimensionless axial coordinate ξ (x/L) and parameter β_i, which depends on the vibration mode studied. Table 1 shows the values of the coefficients for the first vibration mode.

$$y(\xi) = A\,sin(\beta_i\xi) + B\,cos(\beta_i\xi) + C\,sinh(\beta_i\xi) + D\,cosh(\beta_i\xi) \tag{123}$$

Table. 1 Case study of beam with different types of support..

# case	**Case scheme**	$\boldsymbol{\beta_1 L}$	A	***B***	***C***	***D***	**FEM First linear frequency (Hz)**
1 (Roller-roller)		3.14159	1	0	0	0	461.89
2 (Pinned-roller)		3.14159	1	0	0	0	461.89
3 (Pinned-pinned)	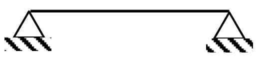	3.14159	1	0	0	0	461.89

4 (Fixed-free)	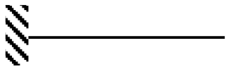	1.87510	1	-1.36222	-1	1.36222	165.81
5 (Fixed-roller)	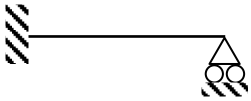	3.92660	1	-0.999223	-1	0.999223	695.14
6 (Fixed- pinned)	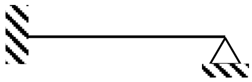	3.92660	1	-0.999223	-1	0.999223	705.47
7 (Fixed-fixed)	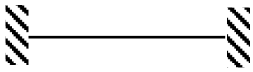	4.73004	-1	1.01781	1	-1.01781	1002.00

3. Results and discussion.

This section presents the results for the nonlinear frequency as a function of the vibration amplitude. First, the analytical results are compared with those reported by other authors and with the numerical results. In addition, seven cases of beams with varying types of end supports, as shown in Table 1, are compared.

3.1 Comparison of the analytical solution with other authors.

Fig. 2 shows the ratio between the nonlinear and linear frequency (ω_{1NL}/ω_1) of the first mode of vibration (nonlinear normal mode, NNM) as a function of the normalized vibration amplitude (a_k). Fig. 2a and Fig. 2b show the pinned-roller case and the roller-roller case, respectively. In Fig. 2a, the solid curve represents Eq. (101), while the blue circles correspond to the FEM results. The results obtained by Luongo [6], are also included for comparison and show strong agreement. Similarly, for the roller-roller case (Fig. 2b), a comparison of the analytical results, the FEM results and the results reported by Wodall 2 [4] is made, showing good agreement among the results.

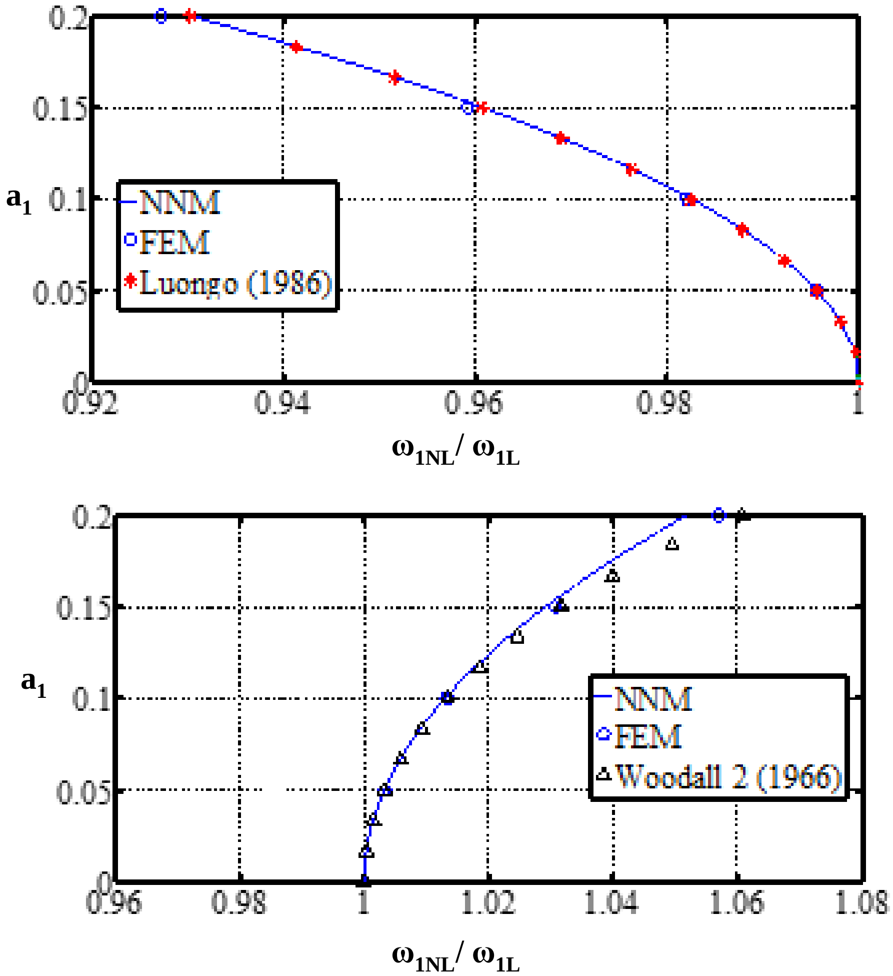

Fig. 2 Frequency ratio-amplitude oscillation for the first NNM pinned-roller (a) and the roller-roller case (b).

3.2 Numerical nonlinear frequency comparison for different supports types

This section analyses the influence of the type of beam support on the nonlinear frequency and vibration amplitude. To do this, the seven cases shown in Table 1 are studied and analysed. Section 2.2 describes the methodology used for the numerical simulation. For each case studied, the oscillation amplitude is gradually increased between 1%-20% of the beam length. For each case studied, seven simulations are performed with 1, 2, 4, 6, 10, 15 and 20% displacements. A total of 49 simulations are carried out in Abaqus, keeping the dimensions and mechanical characteristics of the beam constant. The linear frequency in the seven cases studied is calculated with NLgeom deactivated in Abaqus. In the simulations carried out, the transverse displacement of the central node is monitored at each time increment, which produces a signal whose frequency corresponds to the nonlinear vibration frequency. To accurately calculate the frequency, the Fourier transform is applied. The ratio between the nonlinear and linear frequency of each case is used as a variable for comparison among the seven cases. The frequency ratio in the seven cases plotted against the percent vibration amplitude (Fig, 3) is shown to compare the degree of nonlinearity obtained in the cases studied.

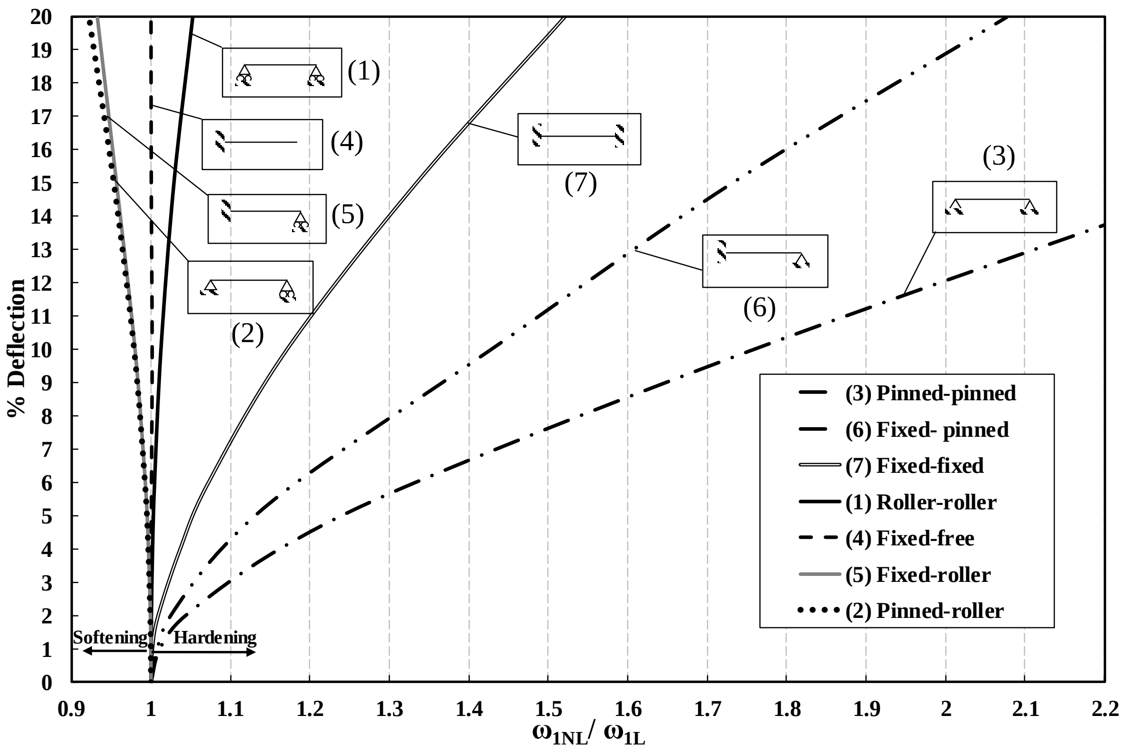

Fig. 3. Numerical result of the frequency ratio-amplitude of vibration for 7 types of beam supports.

The comparative study of the frequency ratio-vibration amplitude curves graphically and simply shows the effect of the support type on the frequency response of the beam when all the mechanical and geometric characteristics of the beam are kept constant. Linear behaviour occurs when the ratio between the nonlinear and linear frequency equals one ($\omega_{1NL}/\omega_1 = 1$). When the frequency ratio is greater than one ($\omega_{1NL}/\omega_1 > 1$), hardening occurs, namely, the stiffness of the beam increases due to nonlinearities; in contrast, if the ratio is less than one ($\omega_{1NL}/\omega_1 < 1$), beam softening occurs, that is, the stiffness of the beam decreases due to nonlinearities. The analysis of the cases studied shows that cases 3, 6 and 7 have greater nonlinearities, which is mainly due to the axial displacement constraint at both supports. The case with greatest nonlinearity is the case with pinned-pinned supports, where pivoting at the ends of the beam is not prevented (case 3). In addition, in this case as well as in other cases in which the axial displacements are constrained at both ends, the degree of stiffness or hardening depends on the slenderness of the beam (λ). This parameter depends on the length, area, and inertia of the beam, as seen in analytical solution Eq (118). The hardening and softening behaviour with the different support types can be fully understood from a detailed analysis of the analytical solutions developed for case 1 (roller-roller) without axial constraints, Eq. (111); for case 2 (pinned-roller) with an axial constraint, Eq. (101); and case 3 (pinned-pinned) with axial constraints at both supports, Eq. (114). In case 3, hardening is always present as slenderness increases since in equation Eq. (116) the nonlinear term is positive (λ) and multiplies the amplitude. In cases 1 and 2, the first term in analytical equations (113) and (103) depends on $(k\pi)^2$, which represents the geometric nonlinearity, producing a hardening effect. Additionally, the second term depends on the factor $(k\pi)^4$ and represents the nonlinearity caused by axial inertia, producing a softening effect. These terms oppose each other due to their opposing signs, and the result defines the behaviour of the beam with the amplitude of vibration; a positive result indicates hardening (the oscillation frequency increases), and a negative result represents softening (the oscillation frequency decreases). As such, case 1 (roller-roller) leads to hardening behaviour and case 2 (pinned-roller) to softening behaviour. This behaviour is demonstrated in the numerical cases shown in Fig. 3. In cases 1 and 2, the ratio between the linear and nonlinear frequencies (ω_{1NL}/ω_1) does not depend on the mechanical properties of the beam; for this reason, only the amplitude term appears in the analytical solution. Moreover, to explain the behaviour of case 6 (fixed-pinned), it is observed that the difference between this case and case 3 is the rotational constraint of one of the supports, and this effect is taken into account in the deflection equation of the beam according to Eq. (123). In case 3, the deflection function is the sine function as show the Eq. (37), conversely in case 6, the deflection has hyperbolic sines and cosines function as shows Eq. (123). The geometric nonlinearity is lower in case 6 and results in less hardening. The behaviour of case 7 (fixed-fixed) is similarly explained since the amount of angular deformation is lower and the hardening is therefore lower than those in cases 3 and 6. Furthermore, the softening behaviour in case 5 (fixed-roller) is similar to that in case 2; however, the amount of softening is slightly lower due to the difference in deflection in Eq. (123). Case 4 (fixed-free) shows practically linear behaviour; the increases in frequency with respect to the linear frequency do not exceed 1%; therefore, the nonlinear effects are practically negligible.

To better understand the hardening and softening behaviour of the two cases with a roller support allowing for axial displacement (cases 1 and 2), a point (or concentrated) mass is added at the end where the roller support is located. The added mass enhances the effects of inertia, and a softening effect is expected due to a frequency decrease caused by the increase in mass. To carry out this study, a point mass whose value is 50% of the mass of the beam is included on each roller support in cases 1 and 2; this value is chosen to obtain results with orders of magnitude similar to those being studied. The procedure is similar to that carried out for the seven previous cases; the mass is included and a simulation for each vibration amplitude considered is performed. The initial displacement imposed is the same as that in the case without mass since the linear vibration mode is still a sine function. Fig. 4, similar to Fig. 3, shows the frequency ratio versus amplitude for cases 1 and 2 with and without a point mass on the roller supports. In case 2, it is observed that the effect of the mass on the end of the beam causes softening, namely, its oscillation frequency decreases approximately 10% with respect to the linear frequency. Regarding case 2, with two roller supports, the effect of the point mass at both ends also causes softening, and the oscillation frequency can be reduced to values lower than the linear frequency; in this case, there is a frequency reduction of up to 7% with respect to the linear frequency for a 20% deflection.

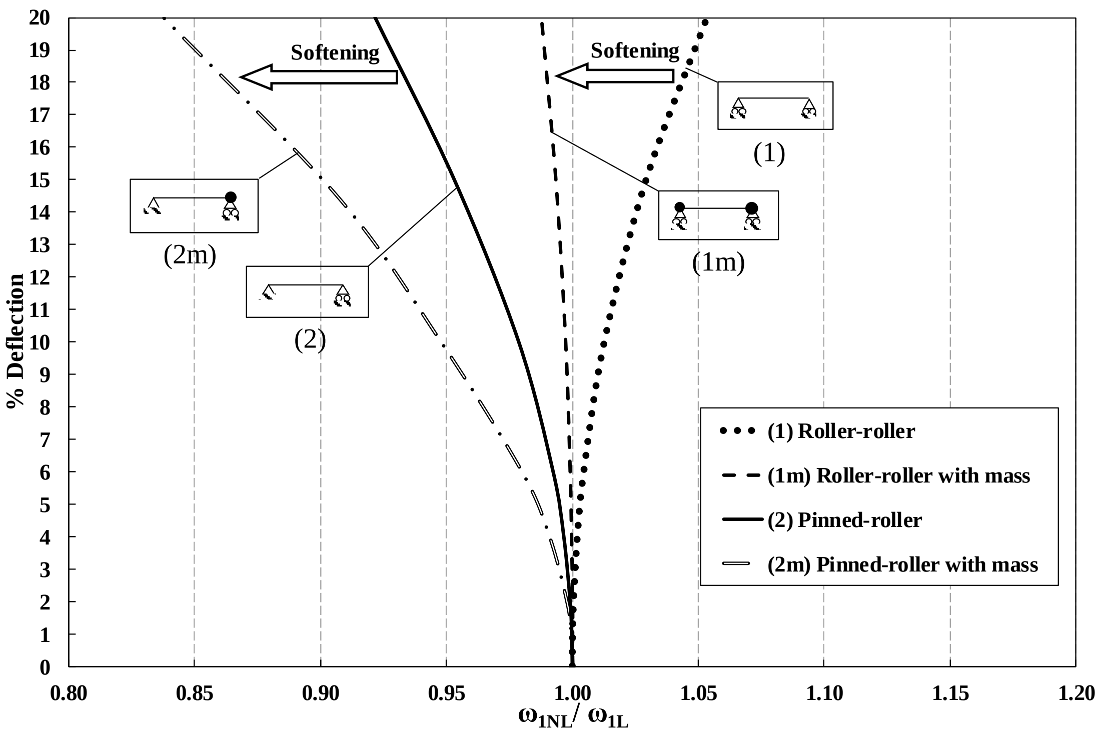

Fig. 4. Numerical result of the frequency ratio-vibration amplitude without point mass, case (1) and (2), and with point mass in the roller support, (1m) and (2m).

4. Conclusion

The main conclusions from the analysis of the results of this study can be summarized as follows.

A detailed analytical study was conducted to find the analytical solution of the nonlinear frequency of a beam with pinned-roller (case 2), roller-roller (case 1) and pinned-pinned (case 3) supports. The equation of motion of the beam section, discretization using NNMs and the multiscale perturbation method were applied to find the analytical solution for the nonlinear frequency. Furthermore, for the cases of the roller-roller beam (case 1) and the pinned-pinned beam (case 3), the same procedures were used, but the boundary conditions at the supports were changed. The analysis of the analytical solutions for case 1 and 2 shows that there are two types of nonlinearities: geometric nonlinearities and nonlinearities due to axial inertia. The geometric term causes hardening by increasing the stiffness of the beam and therefore increasing the vibration frequency of the system. However, the axial inertia term causes softening and therefore decreases the stiffness and vibration frequency. In both cases, the analytical solution does not include the mechanical properties of the beam, and therefore, the solution is independent of these. In contrast, in case 3 (pinned-pinned), the analytical solution does depend on the mechanical properties through the slenderness parameter, which always causes hardening due to the positive sign associated with it, as seen in the analytical solution. The methodology followed is well-known in the literature; however, in this part of the study, an effort was made to show some intermediate results of the calculation to make the procedural steps easier to follow, enabling other studies to replicate those steps. Additionally, the final solution is expressed in such a manner that the geometry-dependent terms and those dependent on axial inertia are clearly shown to facilitate understanding of the physical phenomena of hardening and softening.

Moreover, the objective of the numerical study carried out was to analyse the influence of the types of the beam supports on the nonlinear vibration frequency as a function of vibration amplitude (1-20%). In addition, the analytical solution, the FEM and the solutions of other authors were compared for cases 1 and 2 with satisfactory results. In the numerical comparative study of the cases, the mechanical characteristics of the beam and the amplitude of the oscillations are kept constant to analyse the influence of the type of support. The results show that case 3 presents the extreme case of hardening (pinned-pinned) with 220% for a 20% deflection, followed by cases 6 and 7, and all these cases have axial displacement constraints at both supports. Additionally, case 2 presents the extreme case of softening (pinned-roller) at 10%, where the nonlinearity of the axial inertia exceeds the geometric nonlinearity due to the motion of the roller support. Case 4 is noteworthy since the results show that the behaviour is practically linear despite the large oscillations to which the beam is subjected. In addition, to enhance the influence of axial inertia on the geometric nonlinearity, cases 1 and 2 were modified by adding a concentrated mass on each movable support that allows axial displacement, which resulted in the expected softening and decreased frequency.

Finally, this study may be useful for structural designers, since it provides a clear qualitative idea of the effects of the types of supports on the nonlinear frequencies and enables the modification of the frequency of the system acting on the supports, restricting or allowing movements depending on whether increasing or decreasing the nonlinear frequency is desired.

Regarding future work, this study can be applied to plates and membranes, where vibrations may be important in other directions or in combinations of several directions. Furthermore, the study of plates and membranes can cover a wider field of applications.

5. References

[1] J. J. Thomsen, Vibrations and Stability, New York: Springer, Berlin, Heidelberg, 2003.

[2] Q. Han and X. Zheng, “Chaotic Response of a Large Deflection Beam and Effect of the Second Order Mode,” *European Journal of Mechanics A/ Solids,* pp. 24, 944-956, 2005.

[3] W. Lacarbonara and H. Yabuno, “Refined Models of Elastic Beams Undergoing Large In-plane Motions: Theory and Experiment,” *Int. J. Solids and Structures,* vol. 43, pp. 5066-5084, 2006.

[4] S. R. Woodall, “On the Large Amplitude Oscillations of a Thin Elastic Beam,” *Int. J. Non-linear Mechanics,* pp. 217-238, 1966.

[5] S. Atluri, “Nolinear Vibrations of a Hinged Beam Including Nonlinear Inertia Effects,” *Journal of Applied Mechanics,* vol. 40, pp. 121-126, 1973.

[6] A. Luongo, G. Rega and F. Vestroni , "On Nonlinear Dynamics of Planar Shear Indeformable Beams," *Journal of Applied Mechanics,* vol. 53, pp. 619-624, 1986.

[7] A. H. Nayfeh, C. Chin and S. A. Nayfeh, "Nonlinear Normal Modes of a Cantilever Beam," *Journal of Vibration and Acoustics,* vol. 117, pp. 477-481, 1995.

[8] A. H. Nayfeh and S. A. Nayfeh , "On Nonlinear Modes of Continuous Systems," *Journal of Vibration and Acoustics,* vol. 116, pp. 129-136, 1994.

[9] R. M. Rosenberg, "The Normal Modes of Nonlinear N-Degree-of-freedom Systems," *Journal of Applied Mechanics,* vol. 29, pp. 7-14, 1962.

[10] S. Shaw and C. Pierre, "Nonlinear Normal Modes and Invariant Manifolds," *Journal of Sound,* vol. 150, pp. 170-173, 1991.

[11] A. F. Vakakis, "Analysis and Identification of Linear and Nonlinear Normal Modes in Vibrating Systems, PhD disertation," *California Institute of Technology,* 1990.

[12] G. Kerschen, M. Peeters, J. C. Golinval and A. F. Vakakis , "Nonlinear Normal Modes, Part I: A Useful Framework for the Structural Dynamicist," *Mechanical Systems and Signal Processing,* vol. 23, pp. 170-194, 2009.

[13] L. Kloda, S. Lenci and J. Warminski, "Nonlinear dynamics of a planar beam–spring system: analytical and numerical approaches," *Nonlinear Dyn,* vol. 94, p. 1721–1738, 2018.

[14] E. Mettler, Handbook of Engineering Mechanics, New York: McGraw-Hill, 1962.

[15] D. Thorby, Structural Dynamics and Vibration in Practice, Elsevier, 2008.

[16] H. Wagner, "Large Amplitude Free Vibrations of a Beam," *Journal of Applied Mechanics,* vol. 32, no. 4, pp. 887-892, 1965.

[17] S. Wojciech, M. Klosowicz and W. Nadolski , "Nonlinear Vibration of a Simply Supported, Viscoelastic Inextensible Beam and Comparison of four Methods," *Acta Mechanica,* vol. 85, pp. 43-54, 1990.